Asian Journal of Engineering and Applied Technology
ISSN: 2249-068X (P) Vol. 7 No. S2, 2018, pp.109-115

DOI: https://doi.org/10.51983/ajeat-2018.7.2.905

Numerical Investigation of Slurry Erosive Wear Due to Multiple Particle Impact

Mithlesh Sharma[1], Deepak Kumar Goyal[2] and Gagandeep Kaushal[3]
[1]Mechanical Engineering Department, IKGPTU, Kapurthala, Punjab, India
[2]Mechanical Engineering Department, IKGPTU Main Campus, Kapurthala, Punjab, India
[3]Yadavindra College of Engineering, Punjabi University Guru Kashi Campus, Talwandi Sabo, Bathinda, Punjab, India
E-Mail: mithlesh20@gmail.com
(Received 5 October 2018; Accepted 1 November 2018; Available online 9 November 2018)

Abstract **- In the present work, an attempt has been made to investigate the slurry erosion problem using numerical simulation approach. AISI304 steel has been chosen as the base material for the present study. Performance of AISI304 steel under the range of slurry erosion conditions such as an impact angle and impact velocity of the erodent particles are investigated using laboratory developed slurry erosion test rig. To simulate the similar conditions virtually as available in the hydropower plant, finite element analysis software named as Abaqus has been used. Model has been developed using explicit dynamic solver approach. For correlating the behavior of the material with real time conditions, Johnson cook material model and failure model has been used. To simulate the solid particles impact, general contact penalty method has been adopted. Erosive wear rate is correlated with material removal rate and depth of penetration. It has been observed that the simulated results using Abaqus explicit are in confirmation with the experimental results. Furthermore, to analyze the mechanism of erosion, substrate surface was analyzed with reference to stresses and plastic strains developed by the impact of erodent particles.**
Keywords**: Erosive Wear, Numerical Modeling, Modelling, Explicit**

I. INTRODUCTION

In the present era of developing world, there is a growing need for industrialization. To fulfill this need, industry requires energy sources to cater its demand. In particular demand of electrical energy is increasing rapidly day by day [1-3]. Hydropower being a renewable source of energy has fascinated the attention of researchers worldwide for harnessing its potential to fulfill the increasing demand of energy requirement [4-7]. With increasing dependency on hydropower, more burdens have been put on hydroelectric power plant which has resulted in extensive utilization of available hydro power resources [8-9]. To cater the demand, hydroelectric power plants are running under unfavorable conditions such as under high silt content [10-13]. High silt content in the water leads to extensive material removal from various components of hydraulic machinery [14].

In particular, various components associated with hydro machinery such as turbine blades, labyrinth seals and guide vanes are on the extent of maximum damage by abrasive particles [8-9, 2]. Slurry erosion in hydro power plant is a major concern, particularly in the hydropower plant which are feeded from tributaries originating from Himalayan region, where during rainy season silt content increases in the water (up to 10000 ppm) passing through the turbines [3]. Hydro power plants which are affected by slurry erosion damage in India are Chameri, ManeriBhali–I, NathpaJhakri, Koteshwar and Dehar where amount of damage is very high and it needs break down after every one or two monsoons. Erosive wear resulted in to material loss due to frequent impact of erodent particles at high velocities. Similarly, due to frequent interaction between the surface of turbine component and solid particles, deformation and cutting action causes progressive loss of material from the turbine surface takes place gradually. This has resulted in huge monetary loss, reduced effectiveness, forced outages and repair to the hydro power station situated in the Himalayan region [5]. Therefore it is necessary to identify the erosion mechanism of material which causes degradation of material and measures by which it can be prevented.

Researchers revealed that erosive wear rate is function of various parameters such as impingement angle, impingement velocity, kinetic energy of impacting particle, concentration of slurry, grain size, morphology, substrate hardness, temperature, deformable behaviour and mechanical behaviour of materials.

Earlier investigators had worked on the experimental observations of the slurry erosion condition which causes degradation of the material surface. Modeling of the erosion process follows such experimental work which acts as bench mark for the process. Modeling can be used to interpret existing experimental data, or to extend experimental data to conditions that cannot be tested within current facilities of experimentation.

Various investigator employed modeling and simulation as a tool for analyzing the erosive behavior of the components under real time conditions and it was revealed that such methods are able to create similar conditions which provides good relation to experimental technique and able to evaluate material performance throughout erosion process [21-30]. Most considerably modeling erosion wear can help out design engineers, both in the design of better experimental test facilities, material characterization and improvised design of industrial components / systems.

The long lasting industrial approach is to make use of such models which will be able to predict the best erosion resistant material under the real time conditions such as available in hydro power plant and able to envisage the dilapidation condition under which material removal from the surface took place [21].

In view of the fact that material erosion is a multifaceted in nature, it occurs due to inducement of high plastic strain/strain-rate deformations, inducement of high stresses and strains leads to a condition which causes initiation of damage and further progression of damage ultimately leads to failure of material. To investigate behavior under such conditions, it is important to employ suitable and validated material constitutive models which will able to model erosion process with respect to real time situation.

In the present study, slurry erosion behavior of the target surface was determined by carrying out extensive experimentation. Further an attempt has been made to develop a numerical model which will be able to investigate the slurry erosion behavior of the target surface virtually. Numerical model was developed using finite element analysis software named as Abaqus. This model uses element deletion approach along with Johnson cook material damage model.

The damage initiation and propagation on the solid surfaces is modeled by using multiple particles. Results obtained from the numerical model are further compared using experimental results.

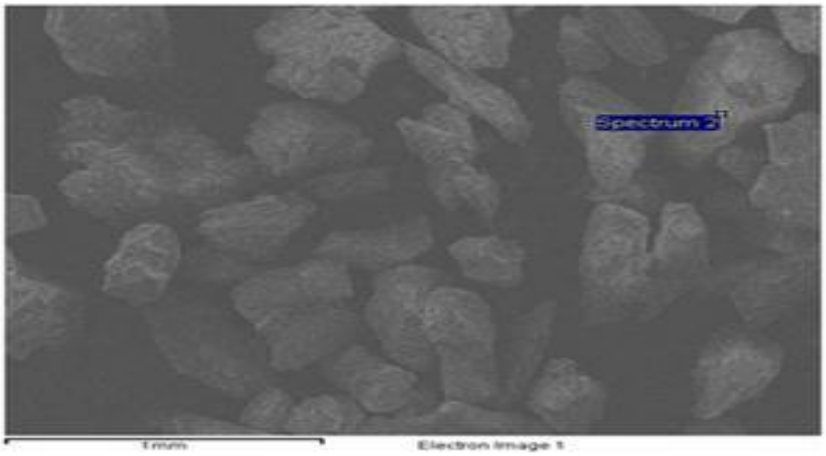

Fig. 1 SEM micrograph of erodent particles

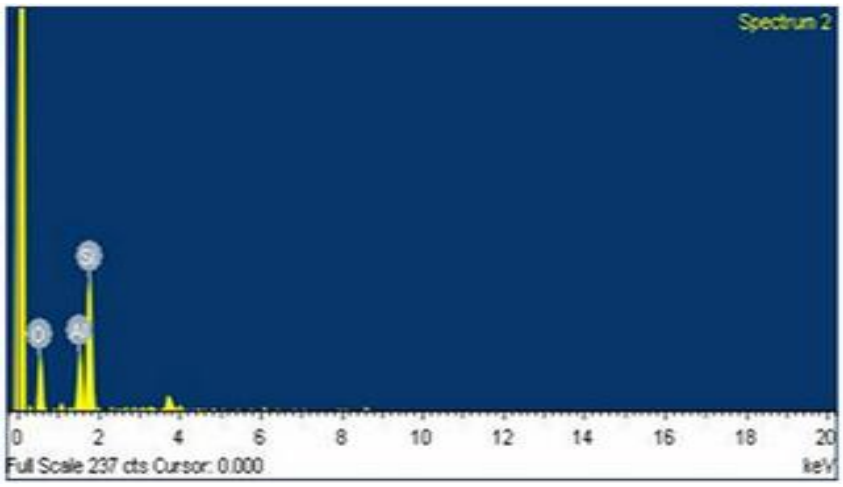

Fig. 2 EDS micrograph of erodent particle

II. EXPERIMENTAL DETAILS

A. Base Material

AISI304 steel is used as base material for the present study. Spectroscopy results of the base material is presented in table I. To characterize the steel micro hardness test using Vickers micro hardness tester was carried out. Hardness reading at ten different locations was taken.

The square samples of side 40 mm with thickness of 8 mm were prepared from given steel.

B. Slurry Particles

Slurry particles for the present study were taken from ManeriBhali stage-1, Hydropower project, Uttarkashi, Uttarakhand, India. Slurry particle taken from hydropower plant was firstly dried under sunlight and sieve analysis was carried out to obtain the particle size. To identify the morphology of erodent particle taken from hydropower plant, Scanning electron microscope (SEM) analysis was carried out as shown in figure 1. Furthermore to identify the various constituents of the erodent particles Emissive Dispersive Spectroscopy (EDS) analysis was carried as shown in figure 2.

C. Slurry Erosion Testing

Experiments were carried out on range of parameters i.e. impact velocity, slurry concentration and average particle size using laboratory developed slurry erosion impact test rig as shown in figure 3. The testing samples were cleaned prior and after the testing with acetone so that no impurities are left over the samples. After testing weight loss measurement was carried out by using weight balance with accuracy of 0.001gram is used. The mass loss per unit time by considering the initial mass loss and final mass loss after testing. Following formula is used for calculating the mass loss.

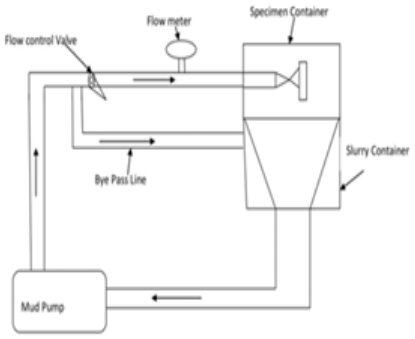

Fig .3 Schematic view of Slurry erosion test Rig

Material Removal Rate (MRR) = $(W_i - W_f)$ / (Unit Amount of Time)
Where W_i is the initial mass of each sample and W_f is the final mass after erosion testing

III. FINITE ELEMENT MODEL AND SIMULATION

A. Finite Element Model

A 3D model of the Substrate has been created using Abaqus/CAE as shown in Figure 4. A small section of 40 × 40 mm has been modeled for analyzing the problem. The Turbine material modeled for present study is AISI304 steel as revealed from the spectroscopy test. The mechanical property for the AISI304 material taken for present study is given in table 2. For simulating the behavior of the erodent particle on the target surface, symmetrically spherical shaped silica particle with 2mm in diameter size is used as erodent particle for impacting the target surface. The mechanical properties for silica sand has been taken as density 1600 kg/m^3, Young's modulus 90.1 GPa and Poisson's ratio 0.25 [6-7].

In the present simulation work, multiple silica particles at an impact angle of 90° and impact velocity 50 m/s impacted on to the target surface. The FEA software named as Abaqus/ Explicit solver was used to compute the impacting phenomena using full integration approach of the elements. Results of the numerical simulation were expressed in terms of Mises stresses, Plastic deformation and value of strain at damage initiation.

Substrate work piece and impacting erodent particle are partitioned into small section by controlling the seed size of the part to obtain the smaller size mesh which result in highly accurate results without carrying out extensive computation. Element types are chosen as explicit method along with mesh deletion element. Mesh deletion element is chosen so as to predict the result which will matches with the real time result. In element deletion mesh, with the impingement of erodent particle on substrate mesh the meshes will started to delete as a result of which material loss from substrate started to takes place. Accuracy of the results depends upon the size of elements. To attain the maximum accuracy in the obtained results by simulation, seed size is controlled to reduce the extensive as shown in Figure 7. C3D8R mesh has been used in present study with eight-node linear brick elements with reduced integration which is able to control the spurious deformation which manifests as a patchwork of zig-zag or hourglass like element shapes, where individual elements are severely deformed, while the overall mesh section is undeformed. This happens on hexahedral 3D solid reduced integration elements and on the respective tetrahedral 3D shell elements and 2D solid elements hour glass control have been used to mesh the target specimen.

TABLE I NOMINAL CHEMICAL COMPOSITION OF THE AISI304 GRADE OF ASTM A240 STAINLESS STEEL (WT.%)

Grade	C_{max}	Si	Mn	P	S	Ni	Cr	Fe
AISI 304 steel	0.02	0.475	1.85	0.40	0.0302	8	18	Balance

TABLE II AISI 304 STEEL PROPERTIES AND THE JOHNSON-COOK PARAMETERS (8)

	Parameter	Units	Value
Mechanical properties	Young modulus,E	MPa	207.8
	Poisson's ratio	-	0.3
	Density,ρ	N/m^3	8000
Physical Properties	Melting temperature,θ_m	Mn	1673
	Transition Temperature, θ_{Trans}	K	1000
	Specific heat capacity	J/KgK	452
	Thermal expansion,α_L	10^{-6} K^{-1}	17.8
Johnson Cook's Strength constant	Initial yield strength, A	MPa	280
	Hardening modulus, B	MPa	802.5
	Strain hardening exponent, n	-	.622
	Thermal softening exponent ,m	-	1.0
	Strain rate const.,C	-	.07999
	Reference strain rate,$\acute{\varepsilon}_o$	1/s	1.0
Johnson-cook fracture constant	d_1	0.69	0.69
	d_2	-	0
	d_3	-	0
	d_4	-	0.0546
	d_5	-	0

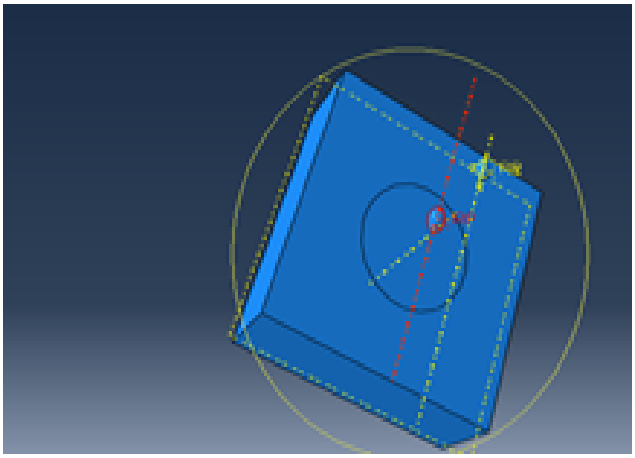

Fig. 4 Target surface and erodent particles view

B. Material Model and Damage Condition

In present study Johnson cook material model has been chosen for defining the base material behavior. This material model is highly recommended for the materials which are facing high strain rate deformations. It deals with material failure and progressive damage during the interaction of erodent particles with the substrate material.

Eqn (1) gives the static yield stress of the material when isotropic hardening is taking place in the material:

$$\bar{\sigma} = \left[A + B\left(\varepsilon^{-pl}\right)^n\right]\left[1 + Cin\left(\frac{\dot{\varepsilon}^{-pl}}{\dot{\varepsilon}_o}\right)\right]\left(1 - \vartheta_m\right) \quad (1)$$

Where A and B are strain hardening coefficients, C is non dimensional sensitivity coefficient of strain rate, m and n represent power of thermal softening and strain hardening respectively. Constants were obtained using split Hopkinson bar test.

The eqn. 2 determines the value of failure or fracture strain which was generated due to impacting of the solid particle on the target surface.

$$\varepsilon_f^{-pl} = \left[d_1 + d_2 \exp\left(d_3 \frac{p}{q}\right)\right]\left[1 + d_4 In\left(\frac{\dot{\varepsilon}^{-pl}}{\dot{\varepsilon}_0}\right)\right]\left(1 + d_5 \vartheta\right) \quad (2)$$

Where p/q is the dimensionless pressure-deviatory stress ratio (p is the pressure stress and q is the mises stress) and θ is the non dimensional temperature. $\frac{\dot{\varepsilon}^{-pl}}{\dot{\varepsilon}_0}$ is the non dimensional plastic strain rate. And d_1, d_2, d_3, d_4 and d_5 are the Johnson cook Failure or fracture constant.

The Johnson cook dynamic failure model evaluates the material failure or damage which has occurred during

impact when the ratio of plastic strain increment ($\Delta\varepsilon^{-pl}$) and (ε_f^{-pl}) failure strain values reaches 1 (ω=1). Eqn.3 shows the damage condition [21]

$$\omega = \Sigma\left(\frac{\Delta\varepsilon^{-pl}}{\varepsilon_f^{-pl}}\right) \quad (3)$$

The Jonson-Cook material damage parameters which are used in present simulation were as follow: d1 = 0.69, d_2 = d3 = d5 = 0, d4 = 0.0546 [9].

C. Boundary Conditions

In the present study target surface was constrained from all the directions in the same manner as in real time situations. Interaction is created by using general contact in Abaqus explicit. Abaqus/CAE does not recognize mechanical contact between part instances or regions of an assembly unless that contact is specified in the Interaction module; the mere physical proximity of two surfaces in an assembly is not enough to indicate any type of interaction between the surfaces.

IV. RESULTS AND DISCUSSION

A. Simulation Results

The simulations were carried out using twenty solid particles. The impingement angles for the erodent particle are taken as 90°. It has been observed that with the impact of first particle, elements of the target surface have failed which verify the fact that damage had taken place due to impact of initial particle. This damage was further propagated for succeeding impingement of the particles. This has been verified by observing the crater profile formed after the impact of the particle as shown in the figure .

In light of the above simulation results, a thorough assessment and more simulations are carried out at the different impingement velocities of 25m/s, 50m/s and 75m/s. These simulation results show that the elements within the contact domain failed because of material damage/failure mechanism. The general contact considers the exposed faces only for the element failure and the underlying elements have not failed.

Thus, the exterior faces of the elements are initially active and the interior faces are initially inactive. Once the exterior element fails, then its faces are removed from the contact domain and the exposed underlying exterior faces become active. This process is progressive for successive impingements. Hence, the general contact between the impinging particles and the target surface coating supports the idea of a damage/failure mechanism [18]. For 25m/s velocity it has been observed that crater area generated at impingement angle of 90° is somewhat lesser then the crater area formed by the impinging particles at impact velocity of 50m/s. It is due to the fact that at higher velocity, high kinetic energy is generated which resulted into higher thrust force which impacted the erodent particles into the coated surface. Similar phenomenon is observed while experimentation that higher mass removal will takes place at higher velocity.

Similarly at higher velocity of 75m/s, more elements of the surface will failed which resulted into higher mass loss as comparison to other velocity. It has been also noticed that when consecutive particles are impinging on the surface of t target surface, particles are rebounded back and divert the coming erodent particle from its path which generate the same phenomenon as reported by the various researcher due to slurry erosion generally known as squeeze film effect. In figure graph has been shown between the stress and time it has been seen that when initially particle is striking on to the surface higher stress will generated and when it is propagated further, it started to decreases.

B. Material Removal Rates

In present study material removal rate is calculated with the help of numerical simulations. In numerical simulation MRR is calculateded with the help of density and mass of the substrate. It has been found that initial mass of the target material was 155.450 grams. It was observed that 25,835 elements are generated on the target surface. Thus mass of each finite elements comes to be 0.0060 grams. The material rate is determined with the help of failed elements in simulations after each run.

The MRR will be computed by multiplying the number of failed elements in given time with mass of each finite element. MRR obtained from simulation were compared with the results obtained by experimentation for 5mins time, as shown in Fig.7. found that FEA based MRR values are in good agreement with the experimentally obtained results. The FEA calculated MRR values are in good agreement with the experimental values.

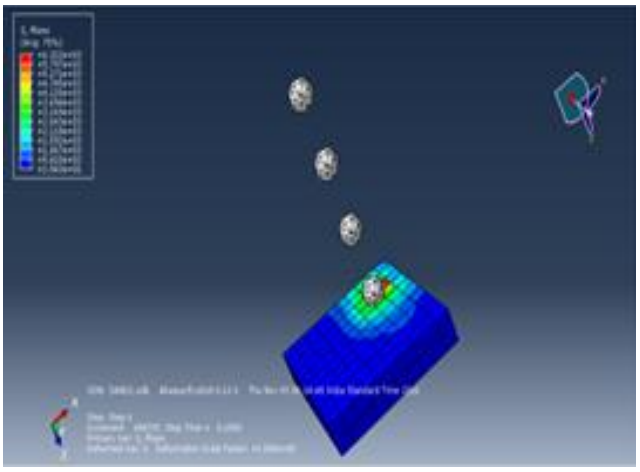

Fig. 5 Contour plot for stress development

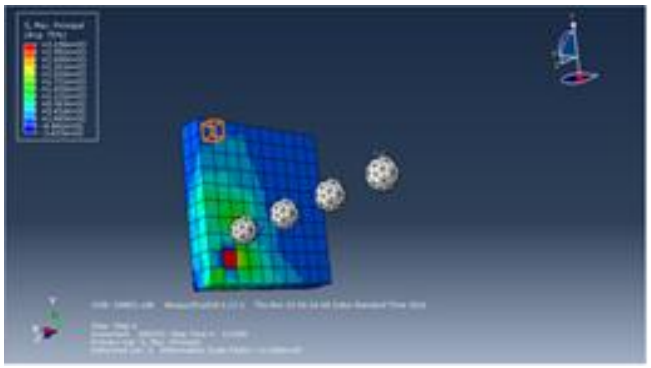

Fig. 6 Contour plot for Plastic strain

Damage of the material takes place when the equivalent plastic strain value in the material exceeds the value of the failure damage in the surface occurred due to the consecutive impingements of the particles as a result of which micro cutting and material removal from the target surface takes place.

V.CONCLUSION

In this investigation a Material failure model was developed using three dimensional FEA software, Abaqus Explicit. In present numerical model Eulerian and Lagrangian approach has been used. In this model FEA concepts such as multiple particle impingement, element deletion and material failure model is used. Model presented in this investigation is able to predict the craters formation during the slurry erosion. It is able to tell us the amount of material deformed on the coating during the process.

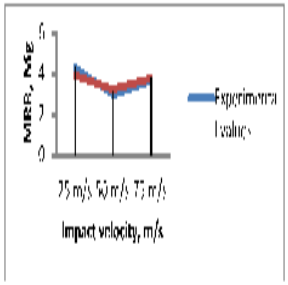

Fig. 7 abagus Explicit

Result obtained using FEA Abaqus Explicit software were compared with the results obtained experimentally. It was found that results obtained were in line with those obtained experimentally. Along with result obtained, the location determined by the simulation results were in coincidence with experimental results. The numerical simulation results verified the fact that extensive experimentation can be reduced with these simulation tests which will result in saving of time and money. These simulation models can be applied to various industries such as hydro power plant, mining, oil, marine, power generation industries etc. it was revealed that failure of material takes place when the strain induced in a material exceed the value of strain at failure.

REFERENCES

[1] T.R. Bajracharya, C.B. Joshi, R.P. Saini and OG Dahlhaug, "Sand erosion of Pelton turbine nozzles and buckets: a case study of Chilime hydropower plant," *Wear*, Vol. 264, , pp. 177-184 2008..

[2] Chawla, V., Sidhu, B.S. Puri, D. and P. Singh, "Performance of Plasma Sprayed Nanostructured and Conventional Coatings," *J. Australian Ceramic Society*, Vol. 44, pp. 56-62. 2008.

[3] B. S. Sidhu, Puri and S. Prakash, "Mechanical and metallurgical properties of plasma sprayed and laser remelted Ni–20Cr and Stellite-6 coatings," *J. Materials Processing Technology*, Vol. 159, pp. 347-355, 2005.

[4] M. Federici, M. Cinzia, A. Moscatelli, S. Gialanella, and G. Straffelini, "Effect of roughness on the wear behavior of HVOF coatings dry sliding against a friction material," *Wear*, Vol. 368-369, pp. 326-334, 2016.

[5] P. Lawrence and E. Atkinson, "Quantitative design and performance prediction methods canal sediment extractors, in International Conference on Irrigation System Evaluation and Water Management-1988, Wuhan, Editor. China," pp. 101-115, 1988.

[6] J.F. Santa, L.A. Espitia, J.A. Blanco, S.A. Romo and A. Toro, "Slurry and cavitation erosion resistance of thermal spray coatings," *Wear*, Vol. 267, pp. 160-167, 2007.

[7] D.K. Goyal, H. Singh, H. Kumar and V. Sahni, "Erosive Wear Study of HVOF Spray Cr_3C_2–NiCr Coated CA6NM Turbine Steel," *Journal of Tribology*, Vol. 136, pp. 041602-613. 2014.

[8] D.K. Goyal, H. Singh, H. Kumar and V. Sahni, "Slurry Erosive Wear Evaluation of HVOF-Spray Cr_2O_3 Coating on Some Turbine Steels," *Journal of Thermal Spray Technology*, Vol. 21, pp. 838-851, 2012.

[9] J.G.A. Bitter, "Study of Erosion Phenomena," *Wear*, Vol. 6, No. 1, pp. 169-190, 1963.

[10] D. Lopez, J.P. Congote, J.R. Cano, A.P. Toro and A.P. Tschiptschin, "Effect of Particle Velocity and Impact Angle on the Corrosion–Erosion of AISI304 and AISI 420 Stainless Steels," *Wear*, Vol. 259, pp. 118-124, 2005.

[11] M.R. Ramesh, S. Prakash,S.K. Nath, P.K. Sapra and B. Venkataraman, "Solid Particle Erosion of HVOF Sprayed WC-Co/NiCrFeSiB Coatings," *Wear*, Vol. 269, pp. 197-205. 2010.

[12] S. Hong, W. Yuping, Q. Wang, G. Ying, G. Li, W. Gao, B. Wang and G. Wenmin, "Microstructure and Cavitation–Silt Erosion Behavior of High-Velocity Oxygen–Fuel (HVOF) Sprayed," *Surface & Coatings Technology*, Vol. 225, pp. 85-91, 2013.

[13] L. Thakur and N. Arora, "A Comparative Study on Slurry and Dry Erosion Behaviour of HVOF Sprayed WC–CoCr Coatings," *Wear*, Vol. 303, pp. 405-411, 2013.

[14] M.S. Mahdipoor, F. Tarasi, C. Moreau, A. Dolatabadi and M. Medra, "HVOF Sprayed Coatings of Nano-Agglomerated Tungsten-Carbide/Cobalt Powders for Water Droplet Erosion Application," *Wear*, Vol. 330-331, pp. 338-347, 2015.

[15] E. Elkholy, "Prediction of abrasion wear for slurry pump materials," *Wear*, Vol. 84, pp. 39-49, 1983.

[16] D.K. Goyal, H. Singh, H. Kumar, V. Sahni, "Slurry Erosive Wear Evaluation of HVOF-Spray Cr_2O_3 Coating on Some Turbine Steels," *Journal of Thermal Spray Technology*, Vol. 21, No. 5, pp. 838–851. 2012.

[17] H.M. Hawthorne, B. Arsenault, J.P. Immarigeon, J.G. Legoux and V.R. Parameswaran, "Comparison of Slurry and Dry Erosion Behaviour of some HVOF Thermal Sprayed Coatings," *Wear*, Vol. 225–229, pp. 825-834, 1999.

[18] B.K. Prasad, A.K. Jha, O.P. Modi and A.H. Yegneswaran, "Effect of Sand Concentration in the Medium and Travel Distance and Speed on the Slurry Wear Response of a Zinc-Based Alloy Alumina Particle Composite," *Tribology Letters*, Vol. 17, pp. 301-309, 2004.

[19] T. Manisekaran, M. Kamaraj, S.M. Sharrif and SV. Joshi, "Slurry Erosion Studies on Surface Modified 13Cr-4Ni Steels: Effect of Angle of Impingement and Particle Size," J*ournal of Materials Engineering and Performance*, Vol. 16, No. 5, pp. 567-572, 2007.

[20] H.Z. Yu, Y.H. Huang and L. Quan, "Erosion Wear Experiments and Simulation Analysis on Bionic Anti-Erosion Sample," *Science China Technological Sciences*, Vol. 57, pp. 646–650, 2014.

[21] Z.G. Liu, S. Wa, V.B. Nguyen and Y.W. Zhang, "Finite element analysis of erosive wear for offshore structure," *13th International Conference on Fracture, Beijing, China*, 2013.

[22] V. Kannojiya, S. Kumar, M. Kanwar and S.K. Mohapatra, "Simulation of Erosion Wear in Slurry Pipe Line Using CFD," *Applied Mechanics and Materials*, Vol. 852, pp.459-465, 2016.

[23] N. Kumar and M. Shukla, "Finite Element Analysis of Multi-Particle Impact on Erosion in Abrasive Water Jet Machining of Titanium Alloy," *Journal of Computational and Applied Mathematics*, Vol. 236, No. 18, pp. 4600-4610, 2013.

[24] B. Yıldırım and S. Muftu, "Simulation and Analysis of the Impact of Micron-Scale Particles onto a Rough Surface," *International Journal of Solids and Structures*, Vol. 49, pp. 1375–1386, 2012.

[25] N.P. Daphalapurka, F. Wang, B. Fu, H. Lu and R. Komanduri, "Determination of Mechanical Properties of Sand Grains by Nano indentation," *Experimental Mechanics*, Vol. 51, pp. 719–728. 2011.

[26] Gu. Xiaoqiang, X. Huang, "Laboratory measurements of small strain properties of dry sands by bender element," *Soils and Foundations*, Vol. 53, pp. 735–745, 2013.

[27] P. Krasauskas, S. Kilikevicius, R. Cesnavisius and D. Pacenga, "Experimental analysis and numerical simulation of the stainless AISI 304 steel friction drilling process," *Mechanika*, Vol. 20, No. 6, pp. 590−595. 2014.

[28] D. Mohotti, T. Ngo and P. Mendi, "Numerical Simulation of Impact and Penetration of Ogvial Shaped Projectiles through Steel Plate structures," *In :ICSECM, India*, pp. 178-183, 2011.

[29] D.K. Goyal, H. Singh, H. Kumar and V. Sahni, "Erosive Wear Study of HVOF Spray Cr_3C_2-NiCr Coated CA6NM Turbine Steel," *Journal of Tribology*, Vol. 136, pp. 041602-12, 2014.